Nuclear Physics A550 (1992) 150-158
North-Holland

NUCLEAR
PHYSICS A

# On gamma decay of giant dipole resonance in tin isotopes

V.Yu. Ponomarev[a,b,1] and A. Krasznahorkay[a,2]

[a] *Kernfysisch Versneller Instituut, 9747 AA Groningen, The Netherlands*
[b] *Faculteit Natuurkunde en Sterrenkunde, Vrije Universiteit, de Boelelaan 1081, 1081 HV Amsterdam, The Netherlands*

Received 24 March 1992
(Revised 18 June 1992)

**Abstract:** The cross sections of excitation of the isovector giant dipole resonance in $^{116,124}$Sn isotopes by inelastic scattering of $\alpha$-particles in coincidence with $\gamma$-decay into the ground state and the first excited $2^+$ state are presented. An attempt has been made to interpret a strong decay into the $2_1^+$ state as a result of coupling of the giant dipole resonance (GDR) with the GDR built on the first $2^+$ state. For that, the microscopic calculation of the GDR fine structure has been performed within the quasiparticle phonon model. The results of calculations are in qualitative agreement with the experimental data.

## 1. Introduction

Recently, coincidence experiments $^{116,124}$Sn($\alpha, \alpha'\gamma$) and $^{208}$Pb($\alpha, \alpha'\gamma$) have been performed at the KVI [1]). The main purpose of these experiments was to determine a neutron skin thickness of nuclei in adjusting the DWBA calculations with different proton and neutron radii ($\Delta R_{pn}/R_0$) to reproduce the absolute value of the measured reaction cross section. The giant dipole resonance (GDR) cross section of excitation by $\alpha$-particles is very small compared to the ones of the giant monopole resonance (GMR) and the giant quadrupole resonance (GQR) which are overlapping with the GDR. To select the contribution of the GDR, coincidence measurements between the scattered $\alpha$-particles and the emitted $\gamma$-rays were performed. One interesting phenomenon has also been observed in these experiments - the population of the first $2^+$ excited state in tin isotopes was nearly as strong as the ground state and practically only the decay into the ground state has been observed in $^{208}$Pb. In the present paper we consider this phenomenon and try to interpret it on the basis of microscopic calculations of the GDR fine structure.

Correspondence to: Dr. V.Yu. Ponomarev, Lab. Theor. Physics, Joint Inst. for Nucl. Res., Dubna, Head Post Office, P.O. Box 79, Moscow, Russian Federation.

[1] Permanent address: Laboratory of Theoretical Physics, Joint Institute for Nuclear Research, Dubna, Head Post Office, P.O. Box 79, Moscow, Russian Federation.

[2] Permanent address: Institute of Nuclear Research of the Hungarian Academy of Sciences, H-4001 Debrecen, Bem tér 18/c, P.O. Box 51, Hungary.

The general idea of such calculations is rather simple. As soon as the GDR is excited by $\alpha$-particles it decays into the ground state by E1 transitions. Since the $\gamma$-decay into the $2_1^+$ state is strong, it might mean that the coupling of the GDR with two-phonon configurations $[\mathrm{GDR}\otimes 2_1^+]_{1^-}$ is sufficiently strong, and we observe E1 transitions from these two-phonon configurations to the first $2^+$ state. The idea of a possible coupling has been proposed earlier [2]). It was applied [3]) within an extended version of the interacting boson model (IBM) to propose measurements of elastic and inelastic $\gamma$ cross sections as a sensitive test of nuclear structure models. These measurements were performed in Illinois [see e.g. ref. [4])] and data were analyzed within the macroscopic dynamic collective model (DCM) [5]) and the IBM. In the present paper we employ this idea for calculations within the microscopic quasiparticle phonon model (QPM) [6,7]) in view of this KVI experiment.

## 2. Details of calculations

Excited states in even–even nuclei are treated by the QPM in terms of the phonon operators $Q^+_{\lambda\mu i}$ with the angular momentum $\lambda$, projection $\mu$ and the RPA root number $i$. The structure of phonons is determined by the contribution of pairs of quasiparticle creation $\alpha^+_{jm}$ and annihilation $\alpha_{jm}$ operators with the shell quantum numbers $jm$ as follows:

$$Q^+_{\lambda\mu i}=\tfrac{1}{2}\sum_{jj'}^{N,Z}\{\psi^{\lambda i}_{jj'}[\alpha^+_{jm}\alpha^+_{j'm'}]_{\lambda\mu}+(-1)^{\lambda-\mu}\phi^{\lambda i}_{jj'}[\alpha_{jm}\alpha_{j'm'}]_{\lambda-\mu}\}\,. \tag{1}$$

Quasiparticle operators appear as a result of the standard Bogoliubov transformation from particle creation and annihilation operators; thus, creation of a particle or a hole is considered as creation of a quasiparticle. To obtain the phonon basis (i.e. the energy of one-phonon configurations and structure coefficients $\psi^{\lambda i}_{jj'}$ and $\phi^{\lambda i}_{jj'}$ in eq. (1)), we solve the RPA equations with an effective hamiltonian including an average field for neutrons and protons, a pairing interaction and a residual interaction in the separable multipole form with the Bohr–Mottelson radial dependence.

To take into account the coupling of simple one-phonon configurations to more complex ones we write the wave function of excited states in even–even nuclei as a mixture of phonon configurations of different complexity (i.e. one-, two-, ...phonon configurations) built on the wave function of the ground state $\Psi_{\mathrm{g.s.}}$, treated as the phonon vacuum. In the present paper, we truncate the basis up to two-phonon configurations and thus, the wave function of the $\nu$th state with angular momentum $\lambda$ and projection $\mu$ has the form

$$\Psi_\nu(\lambda\mu)=\left\{\sum_i R_i(\lambda\nu)Q^+_{\lambda\mu i}+\sum_{\lambda_1 i_1\lambda_2 i_2}P^{\lambda_2 i_2}_{\lambda_1 i_1}(\lambda\nu)[Q^+_{\lambda_1\mu_1 i_1}Q^+_{\lambda_2\mu_2 i_2}]_{\lambda\mu}\right\}\Psi_{\mathrm{g.s.}}\,. \tag{2}$$

As soon as the one-phonon basis is obtained, the interaction matrix elements between one- and two-phonon configurations can be written in terms of the amplitudes $\psi^{\lambda i}_{jj'}$

and $\phi_{ii'}^{\lambda i}$ from eq. (1); thus, no free parameters are used in mixing calculations for these configurations. The coefficients $R_i(\lambda\nu)$ and $P_{\lambda_1 i_1}^{\lambda_2 i_2}(\lambda\nu)$ of the wave function of excited states, eq. (2), and the excitation energies $E_{\lambda\nu}$ yield from diagonalization of our effective hamiltonian. Compared to the macroscopic IBM or DCM mentioned above, we use a more complete phonon basis and the width of the GDR is calculated microscopically, as a result of its coupling to two-phonon configurations. However, we do not take into account many-phonon configurations usually included in the IBM or DCM wave functions.

This approach has successfully been applied to the description of properties of low-lying states and integral characteristics such as position, width and exhaust of the EWSR of giant resonances in medium and heavy nuclei [see e.g. ref. [6])]. Usually, to avoid complicated calculations in the resonance region, the strength function of the E$\lambda$-strength distribution is calculated by means of a well-known technique.

To consider $\gamma$-decay into the $2_1^+$ state we need to know the structure of each $1^-$ state contributing to the GDR. Thus, the fine structure of the GDR has been calculated for the first time. As an example we present in fig. 1 the E1-strength distribution over one-phonon $1^-$ configurations (top) and over the $1^-$ states described by the wave function, eq. (2), (bottom) in $^{124}$Sn. This figure shows the fragmentation of the E1 strength of one-phonon configurations due to the coupling to two-phonon configurations. These types of calculations are rather complicated and certainly are not possible if all configurations, schematically presented in eq. (2), are taken into account. For this reason, we have to truncate the basis in actual calculations, and have included all one-phonon $1^-$ configurations in the range from 10 to 18 MeV and two-phonon configurations made of natural-parity phonons with $\lambda^\pi = 1^- - 6^+$ in the range from 0 to 20 MeV.

In the calculation of the $(\alpha, \alpha'\gamma)$ cross sections we have applied the ideas of the multistep theory of nuclear reactions [see e.g. ref. [8])] and following the procedure described in ref. [9])], deduced the $\sigma_{\alpha,\alpha'\gamma}(E)$ coincidence cross section as:

$$\sigma_{\alpha,\alpha'\gamma}(E) = \sigma_{\alpha,\alpha'}(E)\left[\frac{\Gamma_\gamma(E)}{\Gamma} + \frac{\Gamma^\downarrow}{\Gamma} B_{\mathrm{CN}}(E)\right], \qquad (3)$$

where $\Gamma_\gamma(E)$ is the width of the $\gamma$-decay of an intermediate $1^-$ state into the ground or the $2_1^+$ state and $\Gamma$ is the GDR width. The second term in eq. (3) corresponds to the compound decay, the integral value of which was estimated for the decay into the ground state in ref. [10]) to be 1% in $^{124}$Sn and 6% $^{116}$Sn for the 12–17 MeV excitation energy region. We will return to this term later when discussing the results of calculations.

An essential difference from the phenomenological calculations of $\sigma_{\alpha,\alpha'\gamma_0}(E)$ in ref. [1]) is the following. Using the calculated above structure of the $1^-$ states in the GDR region we can obtain now microscopically both the cross section of excitation $\sigma_{\alpha,\alpha'}(E_{1^-_\nu})$ of each $\nu$th $1^-$ state and its decay width into the ground state or the $2_1^+$ state. The GDR excitation at the KVI energies is dominated by the Coulomb term,

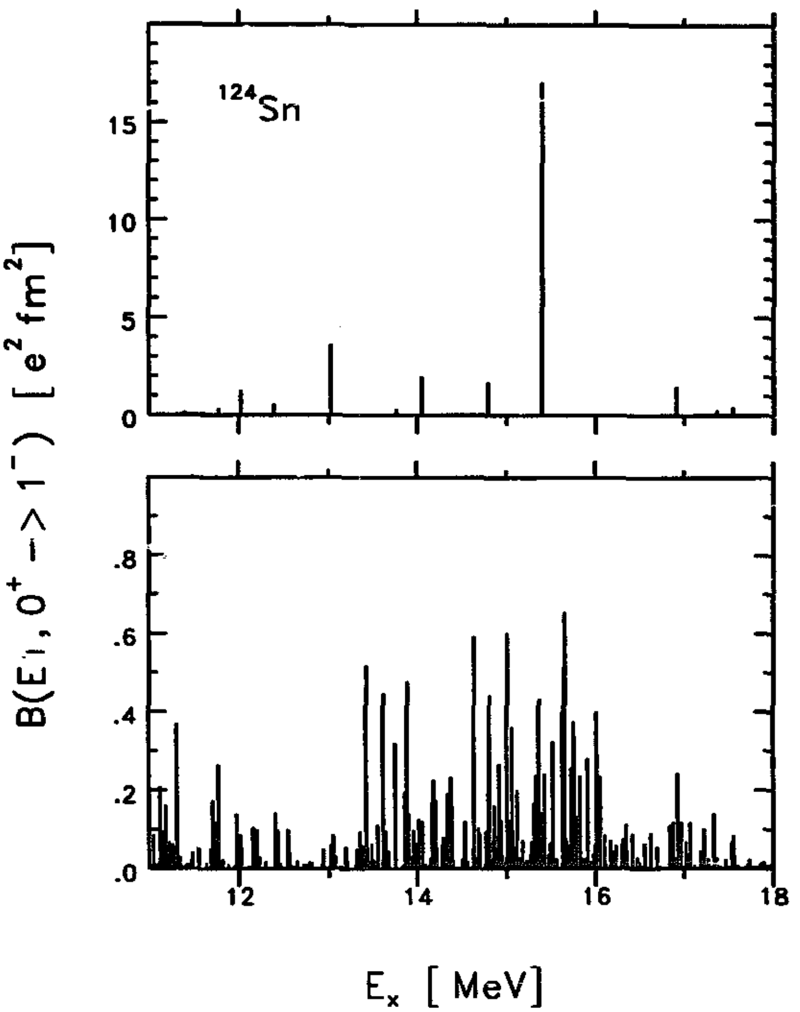


Fig. 1. E1-strength distribution over one-phonon configurations (top) and the strength distribution results from a calculation including two-phonon configuration, eq. (2), (bottom) in $^{124}$Sn.

and the hadronic part of the interaction between a target and a projectile is rather small [11]). Thus, we can approximate the form factor of excitation of the $i$th one-phonon $1^-$ configuration by electromagnetic matrix elements $\langle 1_i^- \| E1 \| 0^+_{g.s.} \rangle$. As we see from the top of fig. 1, the one-phonon configuration at 15.4 MeV carries the main part of the E1 strength and its contribution to the wave function of each $1^-$ state will mainly determine the excitation probability of this state. It has been found [10]) that the excitation $(\alpha, \alpha')$ cross section is practically independent of the particular transition density, Goldhaber-Teller (GT) or Steinwedel-Jensen, used for calculating the transition potential. So we can make an assumption that the role of other weak one-phonon configurations is proportional to their E1 matrix elements. In this scheme we can simplify the calculation of $\sigma_{\alpha,\alpha'}(E_{1^-\nu})$ of the $\nu$th $1^-$ state as follows:

$$\sigma_{\alpha,\alpha'}(E_{1^-\nu}) = \sigma(E) \times \mathcal{N} \times \left| \sum_i R_i(1^-\nu) \langle 1_i^- \| E1 \| 0^+_{g.s.} \rangle \right|^2 , \tag{4}$$

where $\sigma(E)$ is an energy-dependent part of the excitation cross section, determined mainly by the Coulomb excitation, which has an exponential behaviour from the phenomenological calculations with a GT transition density [1]. $\mathcal{N}$ is a normalization factor adjusted to reproduce the integral experimental cross section over the excitation $E_x$ range 12–17 MeV and 13–17 MeV in $^{124}$Sn and $^{116}$Sn, respectively. The absolute value of the cross section has been found to be very sensitive to the difference in the radius of the proton and neutron average field [1]. Since within this theoretical framework we use Woods–Saxon potential with adjustable parameters for the average field, the absolute values of the cross sections are beyond the scope of the present calculation. That is why only the description of the shape of the cross sections and the values of branching ratio between decays into the ground and $2_1^+$ states are considered.

The decay width $\Gamma_\gamma(E_{1^-\nu})$ of the $\nu$th $1^-$ excited state in eq. (3) is simply related to the $\gamma$-transition matrix elements between one-phonon configurations and the phonon vacuum for the decay into the ground state,

$$\Gamma_{\gamma 0}(E_{1^-\nu}) \sim \left| \sum_i R_i(1^-\nu) \langle 0^+_{\mathrm{g.s.}} \| \mathrm{E1} \| 1_i^- \rangle \right|^2 , \tag{5}$$

and between two-phonon and one-phonon configurations for the decay into the $2_1^+$ state,

$$\Gamma_{\gamma 2_1^+}(E_{1^-\nu} - E_{2_1^+}) \sim \left| R_1(2^+1) \sum_i P_{1^-_i}^{2_1^+}(1^-\nu) \langle 2_1^+ \| \mathrm{E1} \| [1_i^- \otimes 2_1^+]_{1^-} \rangle \right|^2 , \tag{6}$$

where $R_1(2^+1)$ is the contribution of the first one-phonon $2^+$ configuration to the structure of the $2_1^+$ state which is equal to 0.95 for both isotopes in the present calculation. In these equations we have omitted terms corresponding to the direct decay from two-phonon configurations to the ground state in eq. (5) and from one-phonon $1^-$ configurations to the one-phonon $2^+$ configurations in eq. (6) which are about two–three orders of magnitude weaker than the main terms [12–15].

Only few two-phonon configurations $[1_i^- \otimes 2_1^+]_{1^-}$ (there are 36 and 39 of such configurations in $^{116}$Sn and $^{124}$Sn, respectively) are involved directly in the GDR decay as we see from eq. (6). All other two-phonon configurations of the wave function (2) play an important role in producing the fragmentation of one-phonon $1^-$ configurations over the states, eq. (2).

## 3. Results and discussions

A typical final-state spectrum is presented for $^{124}$Sn in fig. 2. The experimental methods used for obtaining these data are described in detail in refs. [1,16]. Since the energy resolution of the present experiment was not good enough to resolve the $2_1^+$ state from the ground state, the spectra were fitted by gaussians to separate the $(\alpha, \alpha'\gamma_0)$ and $(\alpha, \alpha'\gamma_{2_1^+})$ cross sections. The result of separating the two $\gamma$-decay

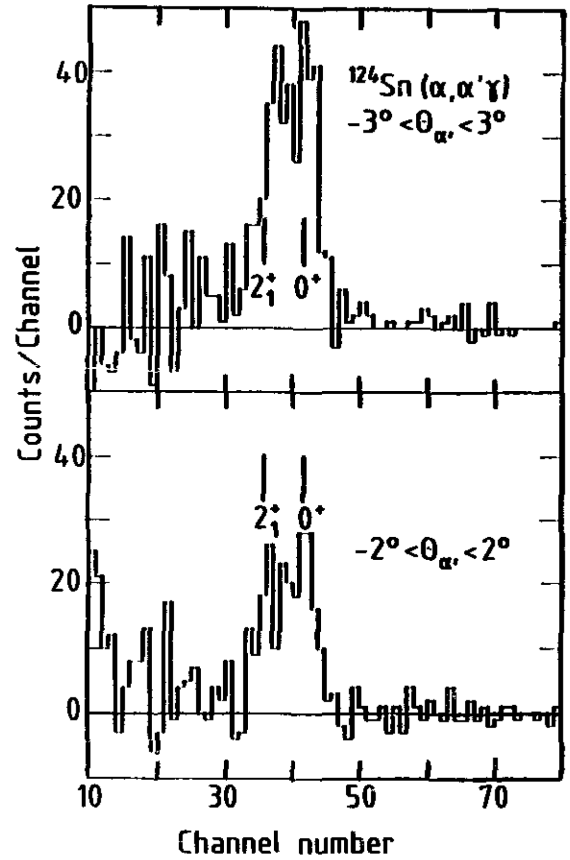


Fig. 2. Final-state spectra of $^{124}$Sn after $\gamma$-decay of the $12 \leq E_x \leq 17$ MeV excitation energy region populated in the $(\alpha, \alpha')$ reaction with $E_\alpha = 120$ MeV and $\Theta_{\alpha'} = 0° \pm 3°$ (top) and $\Theta_{\alpha'} = 0° \pm 2°$ (bottom) after subtracting random coincidences. Lines indicate energy for the $0^+_{g.s.}$ and the $2^+_1$ states.

branches for the region $11 \leq E_x \leq 17$ MeV as a function of excitation energy $E_x$ are shown in fig. 3 together with the results of the QPM calculations for two tin isotopes. The main source of relative errors in data are uncertainties due to statistics, X-ray normalization, and uncertainties in the detection efficiencies of the NaI(Tl) detector and the focal plane system.

In comparing with experiment we have averaged the calculated cross sections, eq. (3), in the following way:

$$\sigma_{\alpha,\alpha'\gamma}(E) = \sum_\nu \sigma_{\alpha,\alpha'\gamma}(E_{1\nu}) \frac{1}{2\pi} \frac{\Delta}{(E - E_{1\nu})^2 + \frac{1}{4}\Delta^2} \tag{7}$$

with the averaging parameter $\Delta = 1$ MeV equal to the bin size used in experimental data in fig. 3.

The calculated cross sections corresponding to the excitation and decay of the GDR are presented in fig. 3 by solid lines. The exponential dependence of the Coulomb excitation cross section as a function of excitation energy enhances strongly lower energies. As a result, the maximum in the $\sigma_{\alpha,\alpha'\gamma_0}(E)$ cross sections is shifted down compared to the E1-strength distribution presented in fig. 1. The increase in

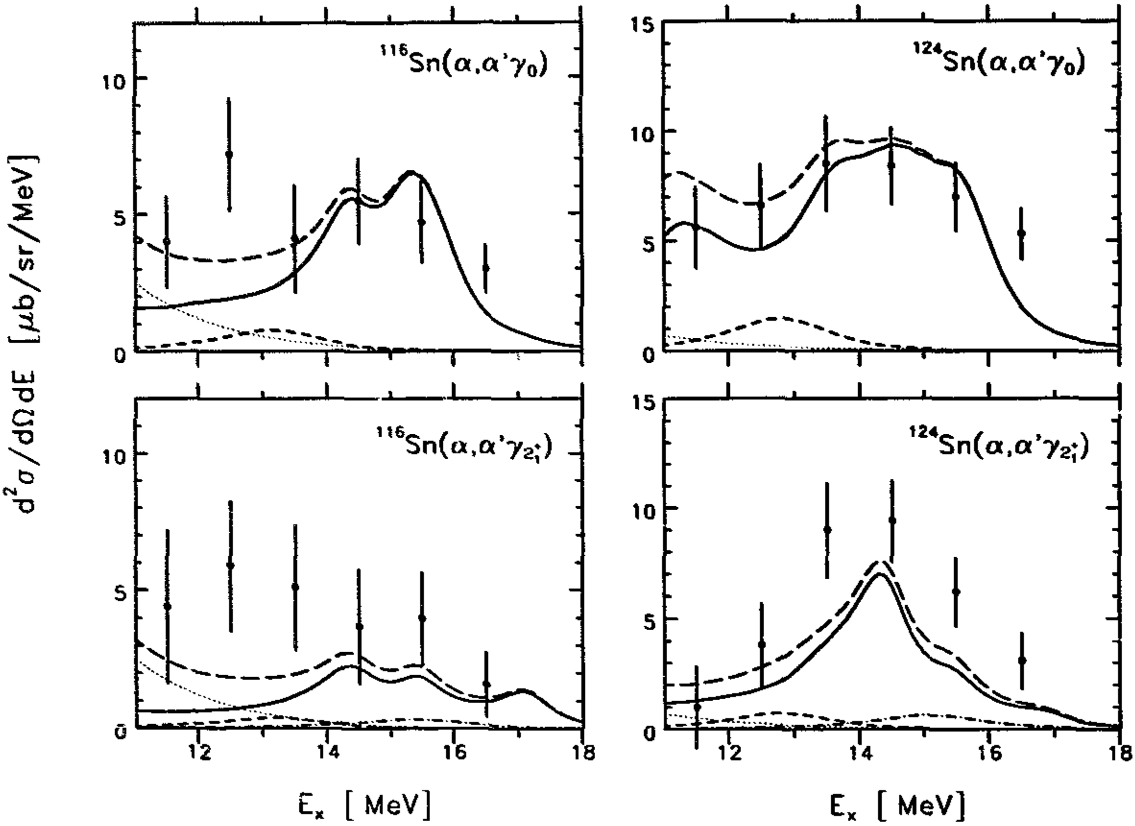


Fig. 3. Measured differential cross section for inelastic α-scattering in coincidence with γ decay into the ground state (top part) and the $2_1^+$ state (bottom part) of $^{116}$Sn and $^{124}$Sn as a function of excitation energy in comparison with the QPM calculations; the solid line corresponds to the excitation of the GDR; dashed line the GQR; dot-dashed line the GMR; dotted line contribution of the compound decay and long-dashed line is the sum of all contributions.

the $\sigma_{\alpha,\alpha'\gamma_0}(E)$ cross sections in $^{124}$Sn around 11.5 MeV is not due to the GDR but is caused by the excitation of some weak one-phonon $1^-$ configurations outside the resonance region. These states are less fragmented because of a lower density of two-phonon configurations around and are enhanced by the Coulomb factor. The two maxima in $^{116}$Sn are due to the fine structure of the GDR. We may expect some other possible contributions to the total $\sigma_{\alpha,\alpha'\gamma_0}(E)$ cross sections from excitation and decay of the GQR at lower energies. Since estimations show this contribution to be relatively small, we did not perform the full microscopic calculations for the GQR, as for the GDR, but estimated it phenomenologically. It has been done following the approach of ref. [1]), with the parameters of the GQR from ref. [17]) and the γ-decay widths of the GQR from the one-phonon calculation within the QPM. The dashed lines in fig. 3 show the contribution of the GQR, the dotted lines are the contribution from the compound decay and the resulting cross sections are presented by long-dashed lines. The shape of the $\sigma_{\alpha,\alpha'\gamma_0}(E)$ cross sections is described rather well without introducing any artificial width of the GDR although the point at 12.5 MeV in $\sigma_{\alpha,\alpha'\gamma_0}(E)$ for $^{116}$Sn is not reproduced in the calculation.

The shape of the $\sigma_{\alpha,\alpha'\gamma_{2_1^+}}(E)$ cross section is very sensitive to the coupling of the GDR with the GDR built on the first $2^+$ state. If the coupling is weak, these two modes exist independently with centroids separated by the energy of the $2_1^+$ state. In this case, the $(\alpha, \alpha'\gamma_{2_1^+})$ cross section is very small. By increasing the coupling we can expect two maxima in the $\sigma_{\alpha,\alpha'\gamma_{2_1^+}}(E)$ cross section from the two aforementioned modes, with the one at higher energy suppressed by the Coulomb factor. This coupling is determined by the collectivity of both the first $2^+$ state and the GDR. To reproduce the collectivity of the $2_1^+$ state we have adjusted the parameter of the isoscalar quadrupole residual interaction to obtain in the calculation the experimental value of the $B(\mathrm{E2}, 2_1^+ \to 0_{\mathrm{g.s.}}^+)$ transition [18]). The collectivity of the $2_1^+$ state in $^{116}$Sn is somewhat stronger as compared to the one in $^{124}$Sn [ref. [18])]. It results in a wider distribution of $\sigma_{\alpha,\alpha'\gamma_{2_1^+}}(E)$ in $^{116}$Sn (see solid lines in the bottom of fig. 3). To estimate phenomenologically the contribution of excitation and decay of the GQR and the GMR that can decay into the first $2^+$ state through the $[2_1^+ \otimes 2_i^+]_{0^+}$ two-phonon configuration, we made an assumption that the coupling of the $2_1^+$ with the GQR and the GMR is the same as with the GDR. They are shown at the bottom of fig. 3 by a dashed line for the GQR and by a dot-dashed line for the GMR. The parameters for the GMR were taken from ref. [17]). We have investigated also experimentally the contribution to the total $\sigma_{\alpha,\alpha'\gamma_{2_1^+}}(E)$ cross section, coming from the GMR. The GMR contributes only to the decay into the $2_1^+$ state and its excitation cross section is strongly decreasing with increasing scattering angle from 2° to 3°. On the other hand, the excitation of the GDR as a function of an angle is practically constant in this range. If the contribution of the GMR is large, the decay ratio for the $2_1^+$ state and the ground state will decrease with increasing angle for the $\alpha$-particles from ±2° to ±3°. As we see from fig. 2, decreasing like that has not been observed experimentally. The shape of the $\sigma_{\alpha,\alpha'\gamma_{2_1^+}}(E)$ cross sections peaking around 14.5 MeV in $^{124}$Sn and practically flat in $^{116}$Sn is reproduced, in general, by the QPM calculations although the amplitudes of these cross sections are underestimated. Again the calculated $\sigma_{\alpha,\alpha'\gamma_{2_1^+}}(E)$ cross section in $^{116}$Sn is smaller around 12.5 MeV than observed. The origin is not clear for us but might be the same as for the $\sigma_{\alpha,\alpha'\gamma_0}(E)$ cross section.

The ratio of the energy integrated $(\alpha, \alpha'\gamma_0)$ and $(\alpha, \alpha'\gamma_{2_1^+})$ cross sections over the energy interval 12–17 MeV can be estimated from the present experiment as $1.5 \pm 0.5$ for $^{116}$Sn and $1.1 \pm 0.3$ for $^{124}$Sn. Our calculations give the values 2.1 and 2.0, respectively.

Concluding, experimental data on the $(\alpha, \alpha'\gamma)$ cross sections for $E_\alpha = 120$ MeV with $\gamma$-decay into the ground state and the $2_1^+$ state have been presented for $^{116,124}$Sn. The data have been analyzed within the quasiparticle phonon model. It has been shown that the major contribution to the coincidence cross section comes from the excitation of the GDR. The decay of the GDR into the $2_1^+$ state is explained by the calculations as a result of mixing of the GDR and the GDR built on the first $2^+$ state. The mixing between these two modes has been calculated microscopically.

The behaviour of the experimental cross sections as a function of excitation energy is described rather well by the calculation without introducing an artificial width of the GDR. But the calculations somewhat underestimate the experimentally observed population of the $2_1^+$ state in comparison with the ground-state population.

Many fruitful discussions with A. van de Woude who suggested the measurements and the discussions of the theoretical interpretation with M.N. Harakeh are gratefully acknowledged. We thank co-authors of paper [1]) for participating in this experiment and O. Scholten for useful comments. One of us (V.Yu.P.) also thanks the Nuclear Physics Groups of the KVI, the Free University of Amsterdam and the NIKHEF for the hospitality during his stay in the Netherlands. This work is part of the research program of the Foundation for Fundamental Research of Matter (FOM) which is financially supported by the Netherlands' Organisation for Scientific Research (NWO).

## References

1) A. Krasznahorkay, J. Bacelar, J.A. Bordewijk, S. Brandenburg, A. Buda, G. van 't Hooft, M.A. Hofstee, S. Kato, T.D. Poelhekken, S.Y. van der Werf, A. van der Woude, M.N. Harakeh and N. Kalantar-Nayestanaki, Phys. Rev. Lett. **66** (1991) 1287
2) A. Bohr and B.R. Mottelson, Nuclear structure, vol. 2, ch. 6-6 (Benjamin, New York, 1975)
3) G. Maino, A. Ventura, L. Zuffi and F. Iachello, Phys. Lett. **B152** (1985) 17
4) S.D. Hoblit and A.M. Nathan, Phys. Rev. **C44** (1991) 2372, and references therein
5) M. Danos and W. Greiner, Phys. Rev. **134** (1964) B284
6) V.V. Voronov and V.G. Soloviev, Sov. J. Part. Nucl. **14** (1983) 583
7) V.G. Soloviev, Prog. Part. Nucl. Phys. **17** (1987) 107
8) H. Feshbach, A. Kerman and S. Koonin, Ann. of Phys. **125** (1980) 429
9) J.R. Beene, F.E. Bertrand, D.J. Horen, R.L. Auble, B.L. Burks, J. Gomez del Campo, M.L. Halbert, R.O. Sayer, W. Mittig, Y. Schutz, J. Barrette, N. Alamanos, F. Auger, B. Fernandez, A. Gillibert, B. Haas and J.P. Vivien, Phys. Rev. **C41** (1990) 920
10) A. Krasznahorkay, J. Bacelar, A. Balanda, J.A. Bordewijk, S. Brandenburg, S.Y. van der Werf, A. van der Woude, M.N. Harakeh and N. Kalantar-Nayestanaki, to be published
11) G.R. Satchler, Nucl. Phys. **A472** (1987) 215
12) P.F. Bortignon, R.A. Broglia and G.F. Bertsch, Phys. Lett. **B148** (1984) 20
13) J. Speth, D. Cha, V. Klemt and J. Wambach, Phys. Rev. **C31** (1985) 2310
14) V.V. Voronov and V.Yu. Ponomarev, Nucl. Phys. **A520** (1990) 619c
15) V.Yu. Ponomarev and V.V. Voronov, Phys. Lett. **B279** (1992) 1
16) T.D. Poelhekken, S.K.B. Hesmondhalgh, H.J. Hofmann, H.W. Wilschut, A. van der Woude and M.N. Harakeh, Phys. Rev. Lett. **62** (1989) 16
17) M.M. Sharma, W.T.A. Borghols, S. Brandenburg, S. Crona, A. van der Woude and M.N. Harakeh, Phys. Rev. **C38** (1988) 2562
18) P.M. Endt, At. Data Nucl. Data Tables **26** (1981) 47